CHEMISTRY
AN ASIAN JOURNAL
www.chemasianj.org

Accepted Article

Title: Step-up synthesis of periodic mesoporous organosilicas with the framework of tyrosine (Tyr-PMOs) and performance on horseradish peroxidase immobilization

Authors: Jianqiang Wang, Wenqi Zhang, Changqing Gu, Wenpei Zhang, Man Zhou, Zhiwei Wang, Cheng Guo, and Linbing Sun

To be cited as: *Chem. Asian J.* 10.1002/asia.201701285

Link to VoR: http://dx.doi.org/10.1002/asia.201701285

A Journal of

ACES
Asian Chemical Editorial Society

A sister journal of **Angewandte Chemie** and **Chemistry – A European Journal**

WILEY-VCH

10.1002/asia.201701285

WILEY-VCH

Step-up synthesis of periodic mesoporous organosilicas with the framework of tyrosine (Tyr-PMOs) and performance on horseradish peroxidase immobilization

Wang Jianqiang*[a], Zhang Wenqi[a], Gu Changqing[a], Zhang Wenpei[a], Zhou Man[a], Wang Zhiwei[a], Guo Cheng*[a] and Sun Linbing[b]

Abstract: A new amino-acid bridged periodic mesoporous organosilicas (PMOs) have been constructed *via* hydrolysis and condensation reactions under acid condition in the presence of template. The tyrosine bissilylated organic precursor (TBOS) was first prepared through multi-step reaction using tyrosine (natural amino acid) as starting material. The PMOs with the framework of tyrosine (Tyr-PMOs) were architected by simultaneously using TBOS and TEOS as complex silicon source in the condensation process. All the Tyr-PMOs materials were characterized by XRD, FT-IR, N_2 adsorption-desorption, TEM, SEM and ^{29}Si solid-state NMR to confirm the structure. The enzyme of horseradish peroxidase (HRP) is first immobilized on these new Tyr-PMOs materials. The optimal conditions of enzyme adsorption are as the followings: temperature of 40°C, time of 8 h, pH of 7. Furthermore, the novel Tyr-PMOs materials could store HRP for about 40 days to keep the enzymatic activity and the Tyr-PMOs-10%-HRP with best immobilization effect could be reused for 8 times at least.

Introduction

Enzymes are commonly used under mild and environmentally friendly conditions as a nontoxic biocatalyst.[1] In the field of green and sustainable chemistry, the utilization of enzymatic catalysis is one of the most promising and rapidly growing areas due to high activity as well as high chemo-, region- and stero-selectivity. [2-4] However, the application of enzymes is inhibited by many factors to show low operational stability and poor reusability because they are easy to denature or inactivate by pH, temperature, organic solvents and detergents. [5-6] In order to effectively solve these problems, many researchers have proved that immobilizing enzyme onto solid supports can overcome these limitations to improve the stability and the efficiency of the enzymes. [7-9] Subsequently, different materials are developed to immobilize enzyme as the solid supports, such as organic materials including chitosan, chitin, collagen or cellulose,[10-12] and inorganic materials including zeolite, ceramics, silica, active carbon or mesoporous materials.[13-17] Among them, mesoporous silica materials have attracted growing research interest as the promising hosts for enzyme immobilization due to high surface area, large pore volume, special pore structure, thermal stability and biocompatibility. [18] Specially, functional mesoporous silica materials with various organic groups show extremely important to immobilize enzyme because of enhancing enzymatic affinity and activity by adjusting the microenvironment of channels. [19]

It is well known that organic groups are usually incorporated within the channels of mesoporous materials via three ways: grafting, co-condensation and periodic mesoporous organosilicas (PMOs). [20] The first two methods of modification can well retain the mesostructure but mesoporous channels are often narrowed or even completely blocked by organic groups to hinder diffusion of enzyme molecules. [21] Compared with these two methods, periodic mesoporous organcosilicas (PMOs) can effectively reduce these shortcomings by using bissilylated organic precursors of type $(R'O)_3Si\text{-}R\text{-}Si(R'O)_3$ (R: organic bridge; R′: methoxy or ethoxy group) to incorporate organic units in the three-dimensional network structure of the silica matrix, which organic units are distributed homogeneouly in the framework and do not occupy pore volume. [22-23] Previous many studies have confirmed that PMOs as an attractive countermeasure provide new opportunities for enzyme immobilization. For example, cytochrome c, xylanase, lysozyme and lipase have been immobilized on PMOs to show better adsorption capacities and stability. [24-27] PMOs can be tuned or be targeted on specific applications due to the different properties in the part “R” of bissilylated organic precursor. Thus, it is important to design the content of “R” to construct kinds of PMOs according to the different requirement. Amino acids are indispensable compounds for human’s body as a source of energy, and play vital roles in many fields including peptide synthesis, biomedical sensors and drug delivery system, etc. They often are immobilized on nanomaterials as promising molecules. [28-31] Among 20 natural amino acids, tyrosine is an aromatic amino acid because of a phenolic group on its side chain. Moreover, tyrosine is an important amino acid in human biological system, which acts as the precursors to various neurotransmitters and thyroxine. [32-33] The phenolic group of tyrosine is also used as the potential binding points to immobilize enzyme because of hydrophilic property in the tyrosine-functionalized materials.

To date, the tyrosine as the part of framework on porous materials has not been reported yet, which spurs us to develop novel amino acid bissilylated organic precursor and construct novel PMOs materials based on the skeleton of amino acid. Thus, in present work, we propose a methodology to architect PMOs materials based on the framework of amino acid and to improve the adsorption properties of PMOs materials for enzyme. This was achieved by co-condensation of tyrosine bissilylated

[a] A/Prof.Wang, Mrs. Zhang, Mrs. Gu, Mr. Zhang, Mrs. Zhou, Mr. Wang, Prof. Guo
College of Chemistry and molecular engineering
Nanjing Tech University
30 Puzhu South Road, Jiangsu, Nanjing, 211816, China
E-mail: jqwang@njtech.edu.cn , guocheng@njtech.edu.cn
[b] Prof.Sun
College of Chemical engineering, State Key Laboratory of Materials-Oriented Chemical Engineering
Nanjing Tech University
Nanjing, 210009, China

Supporting information for this article is given via a link at the end of the document.

organic precursors and inorganic silica source in acid medium using P123 as template. Moreover, tyrosine bissilylated organic precursors were firstly obtained by selecting tyrosine as starting compound via multistep reactions. It should be mentioned here that tyrosine bissilylated organic precursors simultaneously supply two functionalized groups within the framework (urea groups, -NH-CO-NH-) and porous channels (phenol groups, -C_6H_5O) in our materials. These groups derived from natural amino acid molecules could potentially improve affinity ability and immobilization capacity of enzyme. Among the various types of enzymes, Horseradish peroxidase (HRP) was chosen as model enzyme because it is widely employed in the oxidative reactions of many chemicals as an effective biocatalyst. The potential of novel PMO material based on the framework of tyrosine as supports for immobilization of HRP was evaluated and optimized. New bissilylated organic precursors were confirmed by ^{1}H-NMR, ^{13}C-NMR, ESI-Ms and IR spectroscopy. The textural properties of all the synthesized PMO materials were characterized by small-angle X-ray diffraction (XRD), N_2 adsorption-desorption and Fourier transform infrared spectroscopy (FT-IR). These findings should be useful for reasonable creation of new periodic mesoporous organosilica materials according to specific application.

Results and Discussion

Structural characterization of Tyr-PMOs materials

The periodic mesoporous organosilicas (PMOs) materials with the tyrosine as the part of framework were synthesized by varying the concentrations of tyrosine-bissilylated organic (TBOS) precursor in the initial mixture described in the experimental section (scheme 3). The organic precursor of TBOS was first prepared by multi-step reaction using tyrosine as the raw material in scheme 2. All of the compounds including of the intermediates were confirmed by ^{1}H NMR, FTIR and ESI-MS (detailed spectra seen in supporting information). Moreover, the phenolic hydroxyl group in the structure of TBOS was simultaneously introduced into the channels of Tyr-PMOs materials, which is clearly indicated in scheme 1. The structural change and inorganic/organic composition of the Tyr-PMOs–n were accessed by XRD, TEM, SEM, FTIR, Nitrogen sorption and ^{29}Si solid-state NMR. The small angle XRD patterns of the samples Tyr-PMOs-n were indicated in Figure 1. All samples exhibited a sharp and relatively intense diffraction peak assignable to the (100) plane at low *2θ* angles suggesting the formation of hexagonally ordered PMOs. The degree of mesostructural ordering of the Tyr-PMOs framework depends mainly on the concentration of TBOS in the initial sol-gel mixtures. With the increasing amounts of TBOS, the intensity and form of diffraction peak are largely changed in the XRD pattern of Tyr-PMOs. For example, the XRD pattern of Tyr-PMOs-2.5% shows a sharp (100) diffraction peak with *2θ* of 0.86° and two broad diffraction (110) and (200) peaks with *2θ* of 1.48° and 1.70°, which retains well-ordered mesostructural organization. In contrast, the (100) diffraction peak is only observed in the XRD patterns of other materials Tyr-PMOs-7.5%, Tyr-PMOs-10% and Tyr-PMOs-15%. Moreover, the intensity of the (100) peak decreased gradually with the increasing concentration of bissilylated organic precursor TBOS because the phenolic hydroxyl group of TBOS expending within the channels reduced the scattering power of channel wall. This suggests that gradual deterioration of mesostructural order of Tyr-PMOs with the concentration of TBOS increasing, which is partly due to the fact that the compound of TBOS with large molecular size may disturb the formation and self-assembly of surfactant aggregates during the co-condensation process. Simultaneously, addition of the high content of TBOS caused a shift of the (100) diffraction peak to lower *2θ* values, as well as an increasing in *d* spacing and unit-cell constants. In a word, the bissilylated organic precursor TBOS as organic building blocks can successfully form the mesoporous framework in the presence of template surfactant. Furthermore, the amounts of TBOS directly affect on the degree of mesostructural ordering of the PMO framework. Large amounts of TBOS in the pore framework can diminish the mesoporous order of PMO, even resulting in a collapse of the mesoporous structures.

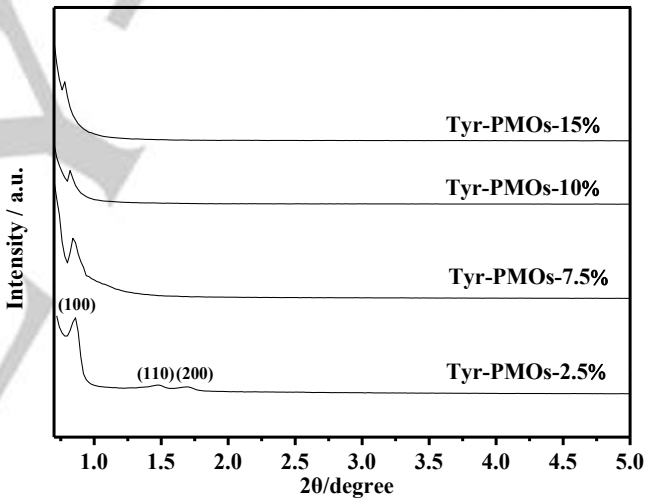

Figure.1 Small angle powder X-ray diffraction patterns of periodic mesoporous organosilicas Tyr-PMOs-n (n=2.5%, 7.5%, 10%, 15%)

TEM and SEM images were used to further elucidate the pore geometry and morphology of these PMOs materials. Figure 2 shows the TEM (left) and SEM (right) images of Tyr-PMOs-n with the different concentration of tyrosine-bissilylated organic precursor. TEM images of all the samples display parallel aligned mesochannels and hexagonal arranged orifices, which clearly indicates the *p6mm* symmetric mesophase. Moreover, All of the materials Tyr-PMOs showed good long range order although a less ordered mesostructure was observed as the content of organic precursor TBOS increasing. These results are consistent with the XRD patterns. With the increasing amounts of TBOS in initial mixtures, the peak intensity of Tyr-PMOs materials decreases, as shown in Figure 1.

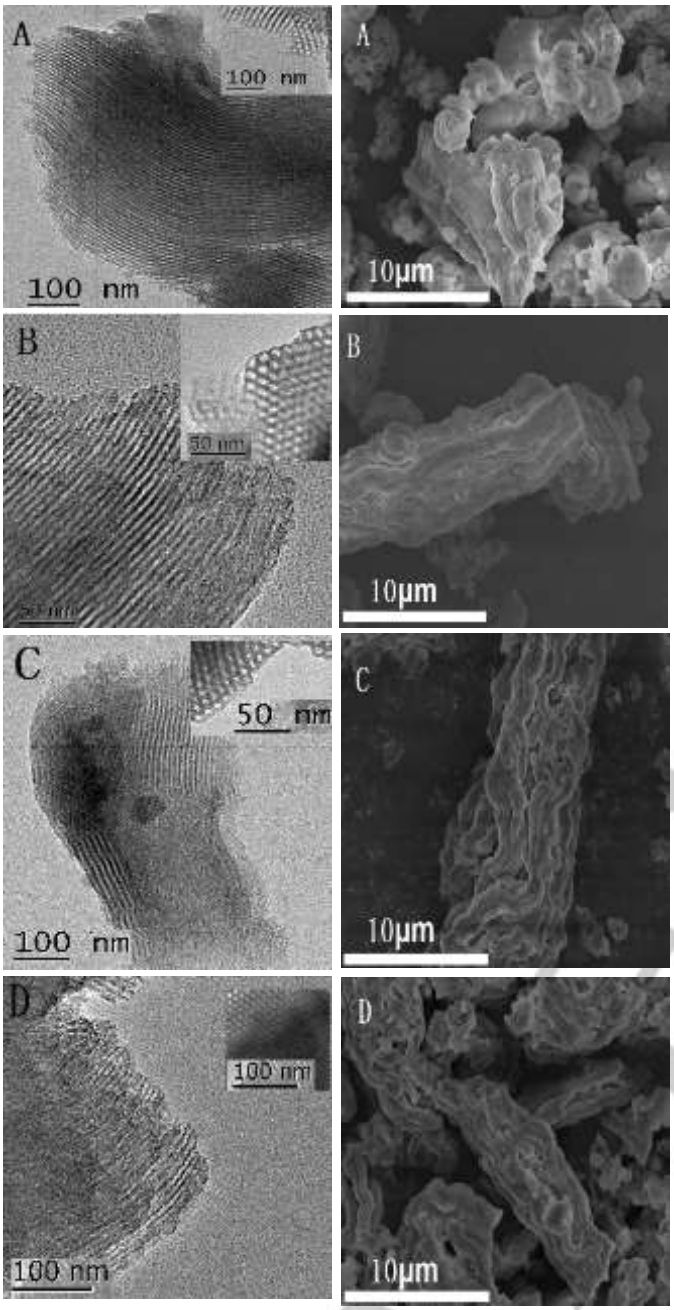

Figure.2 TEM (left) and SEM (right) images of periodic mesoporous organosilicas Tyr-PMOs-n: (A) n= 2.5%, (B) n= 7.5%, (C) n= 10%, (D) n= 15%

SEM images display particle shapes of the materials Tyr-PMOs with the different amounts of organic precursor TBOS. As shown in figure 2, the morphology is largely affected by the adding amounts of the precursor TBOS in initial mixtures. Tyr-PMOs-2.5% shows many twisted morphology aggregating together. However, the rod-like morphology is still observed in the middle conspicuous and bigger particle in figure 2A. The similar rod-like morphology of Tyr-PMOs-7.5% is obviously found to form long threads. These threads assemble for a fiber-like structure along the longitudinal axis. With the increasing amounts of organic precursor TBOS (Tyr-PMOs-10% and Tyr-PMOs-15%), the shapes of primary particles transform to curve threads, which indicates that the organic precursor TBOS improves the flexibility of framework in the materials Tyr-PMOs. Thus, the organic precursor TBOS not only produces the micro-environment of the channels, but also forms flexible and robust morphology of primary particles.

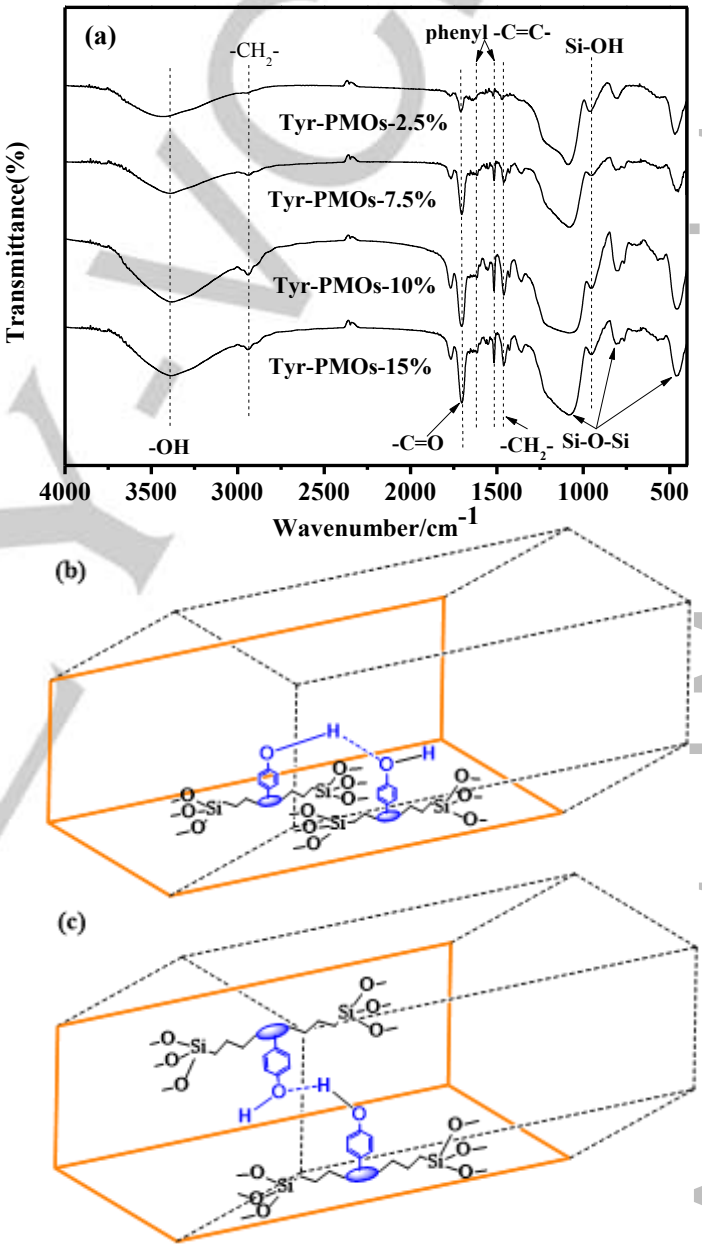

Figure.3 (a) FTIR spectra of periodic mesoporous organosilicas Tyr-PMOs-n (n= 2.5%, 7.5%, 10%, 15%). (b) and (c) Possible assembling formation of hydrogen bond at the pore wall

In order to confirm the chemical bonds and the presence of organic precursor TBOS in the mesoporous walls of Tyr-PMOs materials, FTIR spectra of all the samples were detected after

extracting the surfactant, as shown in Figure 3a. The absorption band at 3380-3430 cm^{-1} can be attributed to O-H stretching vibration of phenolic hydroxyl group. Moreover, the absorption band slightly moves to lower wavelength as the content of organic precursor TBOS increases (For example, the O-H absorption band of Tyr-PMOs-2.5% is 3430 cm^{-1} and that of Tyr-PMOs-15% is 3380 cm^{-1}). Commonly, the change of O-H absorption band is attributed to the formation of hydrogen bond. Thus, the result illustrates that the phenolic hydroxyl group of organic precursor TBOS assembles to form extensive hydrogen bond at the pore wall of Tyr-PMOs materials with high content of organic precursor TBOS. These hydrogen bonds were possibly formed between the adjacent phenolic hydroxyl groups of TBOS molecule at the same side (Figure 3b) or the conjoint two sides (Figure 3c) of the pore wall. The existence of the carbonyl group (C=O) is confirmed by the absorption band located at 1702 cm^{-1} (stretching vibration mode of C=O). Moreover, the stretching vibration bands of C=C in phenyl ring are shown at 1615 and 1515 cm^{-1}. The methylene group (CH_2) is largely observed in the structure of TBOS. The C-H vibration of CH_2 is exhibited at absorption bands at 2940 cm^{-1} (stretching vibration of C-H) and 1458 cm^{-1} (scissoring vibration of C-H), respectively. All of the absorption bands that relate to the groups of TBOS indicate that organic moieties TBOS are successfully anchored within the materials Tyr-PMOs. The intensity of these peaks becomes strong with increasing concentration of TBOS in initial condensation process. Besides, a broad absorption bond at 1080 cm^{-1} is observed on the spectra of all the materials, which indicates the formation of the Si-O-Si framework because the bond is attributed to the asymmetric vibration mode of Si-O. Furthermore, the absorption bands at 806 and 454 cm^{-1} that are assignable to symmetric vibration mode of Si-O and in-plane bending vibration mode of Si-O-Si are also clearly displayed in figure 3. The vibration band for the residual Si-OH appears at absorption band at 954 cm^{-1}. These results indicate that the expected siloxane frameworks are formed in all of the materials Tyr-PMOs with the different content of TBOS.

The N_2 adsorption–desorption isotherms and the corresponding pore size distribution curves of Tyr-PMOs are shown in figure 4. All the samples with different contents of TBOS exhibited type IV adsorption isotherms with capillary condensation according to the IUPAC classification. However, the shape of hysteresis loop shows the different type, reflecting the distinct effect of TBOS contents in initial condensation process on the channel structure of Tyr-PMOs materials. The Tyr-PMOs-n (n=2.5% and 7.5%) materials loaded with lower amounts of TBOS display type IV isotherm with H1 hysteresis loop at high relative pressure with P/P_0 range of 0.6-0.9, which is due to the uniform pore size and structure of these materials. The materials Tyr-PMOs-10% and Tyr-PMOs-15% show the type IV with a clear H4 type hysteresis loop, which demonstrates that mesopore and micropore are simultaneously formed within the channels of these materials. Based on the N_2 adsorption-desorption isotherms, the textural parameters of all the materials are reported in Table 1. With the increasing concentration of TBOS in the framework, a decrease in specific surface area and pore volume was observed in the materials Tyr-PMOs-n, which shows that the functional moieties occupy the mesopore walls. The pore diameter decreased from 7.3 to 5.6 nm with increasing the organosilica loading from 2.5% to 15%. In short, the results of N_2 adsorption-desorption analysis show that Tyr-PMOs-n materials with the framework of TBOS are mesoporous materials with uniform pore distributions, which supplies the possibility of immobilizing HRP molecules.

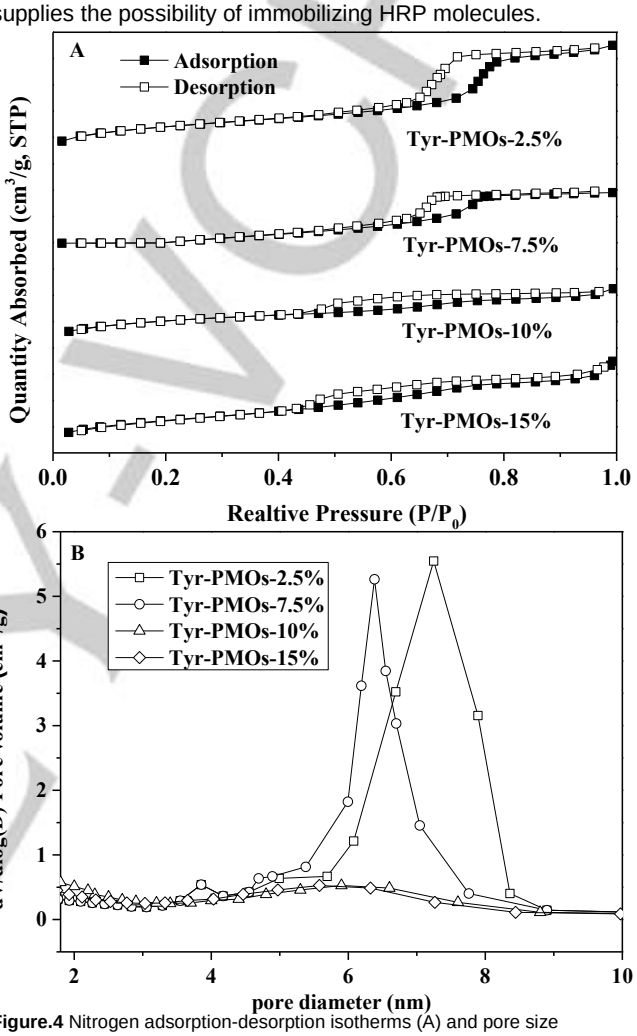

Figure.4 Nitrogen adsorption-desorption isotherms (A) and pore size distribution curves (B) of periodic mesoporous organosilicas Tyr-PMOs-n (n= 2.5%, 7.5%, 10%, 15%)

Table.1 Textual parameters of periodic mesoporous organosilicas Tyr-PMOs-n

Sample	d_{100}[a] (Å)	α_0[b] (Å)	S_{BET} (m^2/g)	Pore volume (cm^3/g)	Pore diameter[c] (nm)
Tyr-PMOs-2.5%	102.7	118.6	549	0.78	7.3
Tyr-PMOs-7.5%	105.2	121.5	338	0.35	6.4
Tyr-PMOs-10%	107.7	124.4	279	0.15	5.9
Tyr-PMOs-15%	113.3	130.8	212	0.10	5.6

[a] Interplanar spacing of the (100) plane, as obtained from the XRD analysis. [b] The α_0 is unit cell parameter, calculated from $\alpha 0=2d_{100}/\sqrt{3}$. [c] Pore diameter is calculated using the BJH model based on the desorption branch of the isotherm.

Figrue 5 displays the ^{29}Si solid-state NMR spectra of the Tyr-PMOs-n materials with the different concentration of organic precursor TBOS. Both Q and T sites corresponding to Q^n (Q^n = $Si(OSi)_n(OH)_{4-n}$, n=2-4) and T^m (T^m = $RSi(OSi)_m(OEt)_{3-m}$, m=2, 3) [34] were clearly observed in these spectra. The chemical schifts of Q^4, Q^3 and Q^2 were designated at -110 ppm, -102 ppm and -91 ppm, respectively. The T signals arising from the organic functional parts of bridged organosilane were obtained in the range of -50 ppm to -70 ppm, which were assigned to the T^3 at -67 ppm and T^2 at -59 ppm. Based on normalized peak areas, the ratio of $T^m/(T^m+Q^n)$ is around 0.094, 0.171, 0.214 and 0.227, which is related to the materials Tyr-PMOs-n (where n = 2.5%, 7.5%, 10%, 15%), respectively.Generally, the Q signals imply the degree of TEOS cross-linking. And the T signals confirm the stability of Si-C bond. As the content of TBOS increases, the intensity of Q signals become weak and the intensity of T signals become strong. These results indicated that the organic moities TBOS were incorporated in the silica network of the Tyr-PMOs materials.

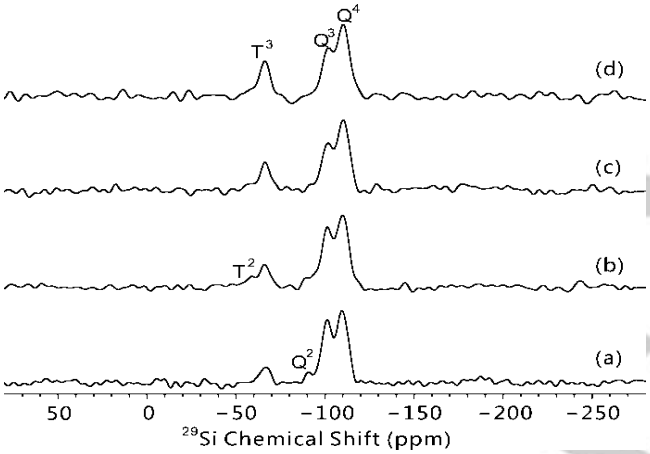

Figure.5 ^{29}Si solid-state NMR spectra of periodic mesoporous organosilicas Tyr-PMOs-n: (a) n= 2.5%, (b) n= 7.5%, (c) n= 10%, (d) n= 15%

Effects of different conditional parameters on HRP immobilization

In addition of the textural parameters of adsorbents, three important factors of immobilization pH, time and temperature determine the adsorption amounts of enzyme. Figure. 6 indicates that the pH affects the adsorbed amounts of HRP on Tyr-PMOs materials. Because pH alters the ionization degree of the functionals groups of the enzyme and the surface charge of the adsorbents, the pH directly influences the adsorption amounts and effectiveness of HRP [35]. Moreover, when the pH is close to the isoelectric point (pI) of enzyme, the adsorbed enzyme can come up to the maximum amounts on the adsorbents [36]. As shown in figure.4, the optimum pH value of absorbed HRP was 7, and the adsorbed amounts were relatively low at the other pH value. At the immobilization pH of 7, the net charge of the enzyme HRP was positive (pI～8.9) while that of the support surface was negative (pI of silica ～2). Thus, high electrostatic attractions were obtained which would enhance the HRP binding onto all of the Tyr-PMOs materials at pH 7.

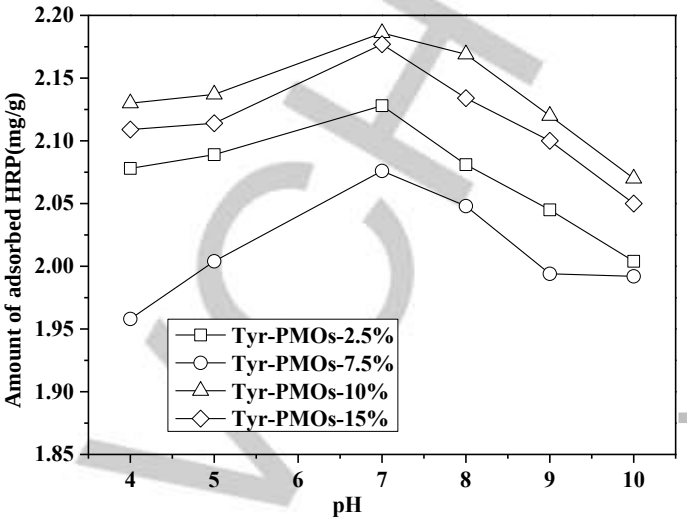

Figure. 6 Effects of immobilization pH of the buffer solution on HRP immobilization

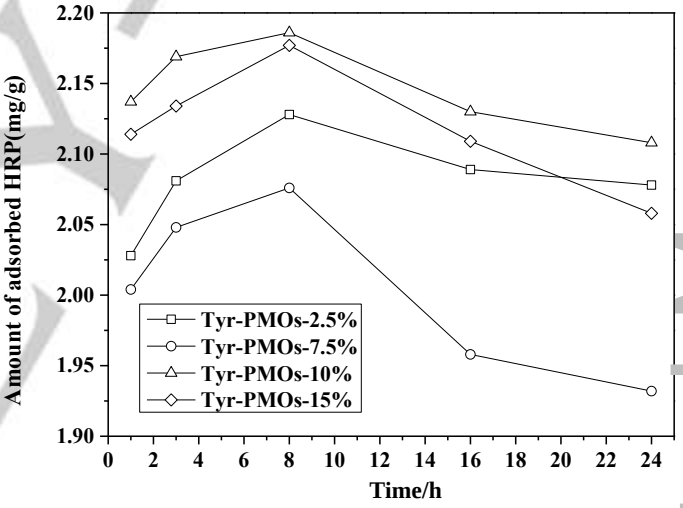

Figure.7 Effects of immobilization time on HRP immobilization

Figure. 7 depicts the effect of time on HRP adsorption onto Tyr-PMOs materials (pH 7.0). As can be seen from the Figure 7, the amounts of absorbed enzyme were increased along with the extension of time. When the immobilization time was 8h, the amounts of immobilized enzyme reached the adsorption equilibrium and no longer increased over time. On the contrary, when the immobilization time was more than 8 h, the amounts of immobilized enzyme decreased. Presumably , the possible reasons can be explained as follows: Firstly, When the loading time is relatively short, the enzyme HRP molecules is attached into the channels of support, but fail to achieve saturation, causing small amounts of immobilized enzyme HRP. When the absorption time is long enough, the HRP molecules have been immobilized onto the surface of supporter channels at saturation coverage, leading to maximum amount of absorbed enzyme. However, the long absorption time gives multiple complicated binding of HRP molecules on the surface of carrier channels,

therefore changing the enzyme's subspace structure, which leads the declination of adsorbed enzyme amounts. When binding sites of the carrier near or have achieved saturation, the total amount of immobilized enzyme can no longer increase due to constant amount of the carrier. Secondly, the long absorption time may cause the HRP molecules leach from the sorbents, thereby decreasing the amount of immobilized enzyme logically. Thus, the optimized adsorption time of HRP is 8h on the Tyr-PMOs materials.

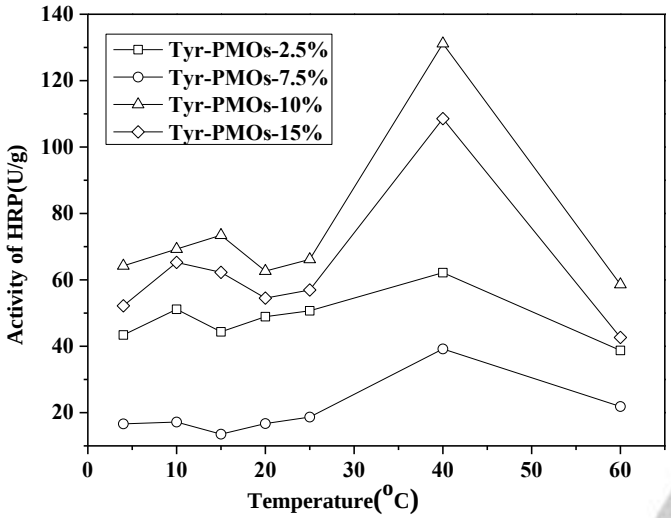

Figure.8 Effects of immobilization temperature on HRP immobilization

Adsorption isotherms of the HRP immobilized on Tyr-PMOs materials at different temperature were showed in Figure. 8. As we can see from Figure. 8, with an increase of temperature, the overall trend of immobilized enzyme's activity showed a slow rise within the temperature range of 20-40°C, but the trend is up and down. The optimum adsorption temperature for the immobilization of HRP was 40°C, at which, the activity of the enzyme reached maximum. Within the temperature range of 40-60°C，the activity of HRP enzyme decreased. It is well known that the increase of the temperature is beneficial to the coupling of the HRP enzyme to the carrier. Besides, an increase of the temperature may accelerate the molecular motion of the HRP enzyme. However, too high temperature may induce irreversible deactivation of enzyme. To summarize, the supporter shows the best adsorption ability owing to the specific micro-environment within the channels, which the better adsorption temperature of HRP enzyme is 40°C on the surface of the Tyr-PMOs materials. Based on these results, the optimized conditions of HRP enzyme are immobilized on Tyr-PMOs-n materials at pH of 7.0 for 8h, and the temperature of 40°C is chosen.

Besides these immobilization parameters, pore structural characters of Tyr-PMOs-n materials are also very important factor of HRP immobilization. As shown in these figures, the adsorption amounts of HRP relate to the concentrations of TBOS in the framework of Tyr-PMOs-n materials. In general, it is clearly seen that the higher immobilization efficiency of Tyr-PMOs-10% and Tyr-PMOs-15% with high content of precursors was observed in all figures though their surface area and pore volume as well as pore size decline. Generally, the size of the HRP molecule is 3.7 nm *4.3 nm *6.4 nm [37]. However, the pore size of Tyr-PMOs-10% and Tyr-PMOs-15% are still able to accommodate HRP molecules in their mesoporous channels because the HRP molecule is elongated, and more amounts of HRP are immobilized on the two samples. Thus, we speculate that the result is probably due to the conformational flexibility of enzyme molecule. In addition, the organic group of phenolic hydroxyl group was simultaneously induced into the channels at the preparation of Tyr-PMOs materials. Moreover, the phenolic hydroxyl group largely added the binding power through hydrogen-bonds to prevent the leaching of HRP enzyme, as shown in scheme 1. The materials of Tyr-PMOs-n (n=2.5%, 7.5%) can absorb HRP molecule easily due to the low diffusion resistance of broad pore structure. However, the adsorbed

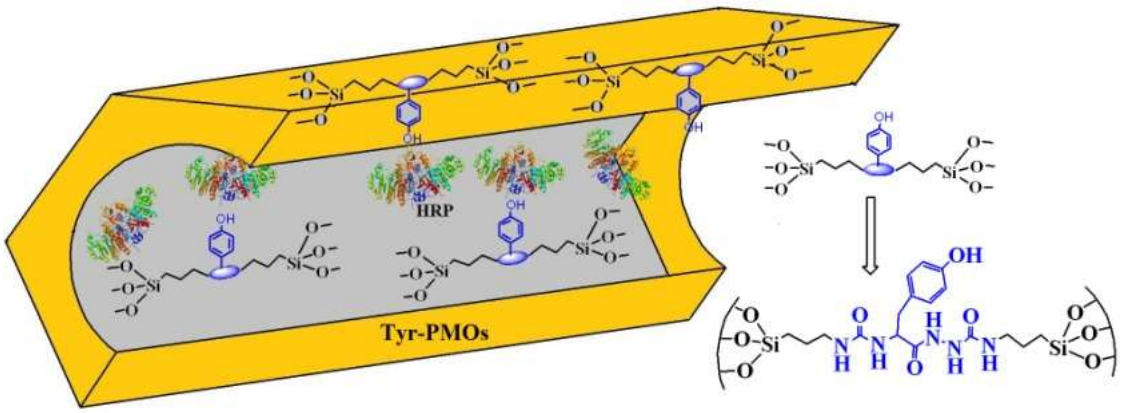

Scheme 1 Possible mechanism of HRP loading in the channel of Tyr-PMOs

amounts of HRP on the two PMOs materials are lower than one of the PMOs materials with high concentrations of TBOS because of less organic group to anchor the HRP enzyme. To sum up, all the above factors produce complicated impact on the loading efficiency of HRP enzyme, and they are interdependent in the whole process.

Stability of Tyr-PMOs-n after the immobilization of enzyme HRP

Figure 9 and Figure 10 show the storage stability and operational stability of immobilizing HRP enzyme, respectively. The Stability of Tyr-PMOs-n-HRP is one of the key factors for large scale applications. Storage stability of Tyr-PMOs-n-HRP with the biggest HRP immobilization amount at room temperature was evaluated after different storage times. (see Figure. 9). The results show little change in the activity of HRP immobilized on the Tyr-PMOs materials with the increasing time. However, it is obvious that the denaturation of immobilized HRP is likely to increase because of long storage time. Specifically, the activity of immobilized HRP had no changes basically within 10 days. After 10 days, a little amount of enzyme will drain out of the channels of Tyr-PMOs materials. Accordingly, it is better to use Tyr-PMOs-n-HRP within 10 days.

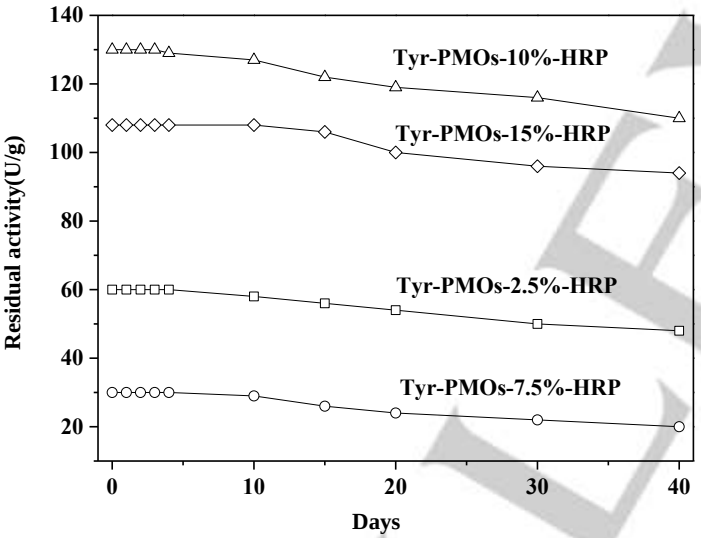

Figure. 9 Storage stability test of Tyr-PMOs-n-HRP with the biggest HRP immobilization amount at room temperature

Operational stability test of screened Tyr-PMOs-n-HRP with the best HRP immobilization effect is demonstrated in Figure. 10. The immobilized HRP can be reused after recovering the sample Tyr-PMOs-10%-HRP from the action solution by simple centrifugation. As shown in Figure 10. That the activity of immobilized HRP decreased with the number of recycling runs, but fortunately still kept 70% of their original activity after the fourth run. The result shows that the immobilized enzyme possesses appropriate stability. Starting from the sixth run, the activity decreased sharply, only 30% of initial activity. The reduction in the activity of HRP in recycling experiments might be caused by the following reasons: One is the slightly release of enzyme HRP that was loosely immobilized from the support, and another is the loss of small quantities of enzyme during reuse and washing operations.

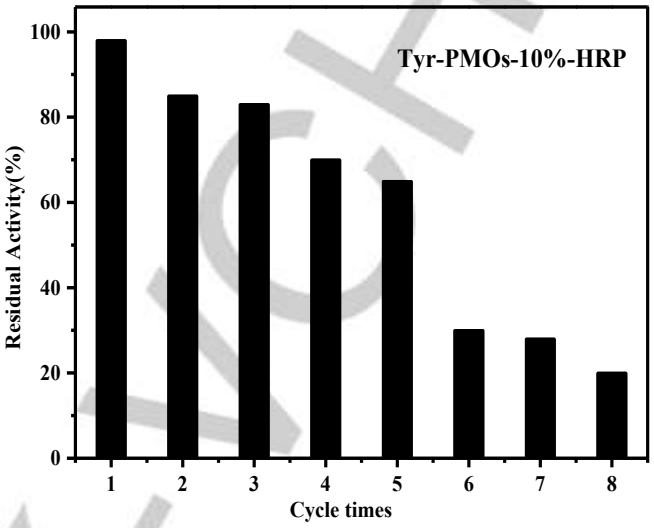

Figure. 10 Operational stability test of Tyr-PMOs-10%-HRP

Conclusions

The experimental results obtained in the present work revealed some conclusive remarks, as follows:

(1) Tyrosine, a natural amino acid, is first used as starting material to successfully prepare a novel bridged organosilicas precursor TBOS by multi-step reactions.

(2) New periodic mesoporous materials with the amino acid as the framework have been constructed by a one step co-condensation of TEOS and Tyrosine bissilylated organic precursorunder the template. Through controlling the proper proportion of organic precursor in the silica source, the resulting samples Tyr-PMOs can still possess the well-ordered 2D hexagonal mesoporous structure. All the Tyr-PMOs materials with the different contents of TBOS are fully characterized by XRD, BET, FT-IR, TEM, SEM and ^{29}Si solid-state NMR.

(3) HRP can be absorbed in various Tyr-PMOs-n materials. Among them, Tyr-PMOs-10% showed the higher immobilization efficiency. The optimum immobilization conditions are as follows: temperature of 40℃, time of 8 h, pH of 7. In this way, one could store enzymes for a longer time (about 40 days) and the Tyr-PMOs-10%-HRP with best immobilization effect could be reused for 8 times at least.

The conclusions obtained in this work may play a significant role in the understanding of enzyme absorption in this kind of new periodic mesoporous organosilicas (Tyr-PMOs), which the material will be undoubtedly useful for their future applications in the fields of biocatalysis or biosensors.

Experimental Section

Regents and chemicals

Horseradish peroxidase was purchased from Aladdin. Triblock poly(ethylene oxide)-poly(propylene oxide)-poly(ethylene oxide) copolymer Pluronic P123 (EO20PO70EO20, Mw=5800) was obtained from Sigma-Aldrich. (3-isocyanato-propyl) triethoxysilane (IPTES) and tetraethoxysilane （TEOS） were the products of Aladdin. Other reagents and solvents were commercially available at analytical grade and used as purchased without further purification.

Synthesis of Tyrosine-bissilylated organic precursor (TBOS)

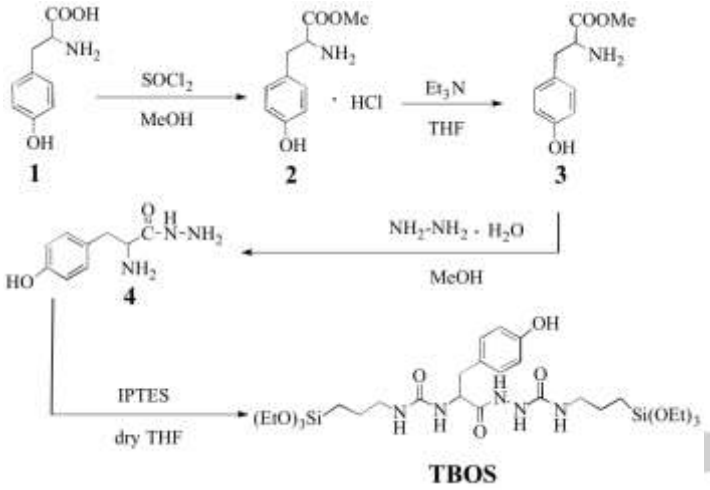

Scheme 2. Synthesis of tyrosine-bissilylated organic (TBOS) precursor

Tyrosine-bissilylated organic (TBOS) precursor was synthesized by the route of scheme 2. First, a suspension solution was formed by mixing tyrosine 1 (11.78 g, 65.00 mmol) and methanol solution (250 mL) in an ice bath. Then, thionyl chloride (5.20 ml, 71.50 mmol) was dropwise added to the above solution. The solution became clear after the addition of thionyl chloride. Next, the reaction mixtures were transferred into oil bath and refluxed overnight at 80 ℃. The solvent was removed under reduced pressure to give crude product of tyrosine methyl ester hydrochloride 2, which are yellowish white solids. Compound 2 was directly used in the following step without further purification. Second, Compound 2 (5.70 g, 23.20 mmol) was immersed in tetrahydrofurane (75.00 mL). Triethylamine (2.35 g, 23.2 mmol) was then added. The mixture was stirred at room temperature for one night. Then, the mixtures were filtered to eliminate the precipitate of triethylamine chloride. The tetrahydrofurane was evaporated obtaining L-Tyrosine methyl ester 3 (dark-white colour, yield of 71%). Third, Hydrazine hydrate (80%, 30 mL) was added to a solution of 3 (2.02g, 10.3 mmol) in methanol (50 mL) at room temperature. The reaction mixtures were stirred for 24 h at the same temperature and subsequently concentrated under reduced pressure. The residue was purified by recrystallization with methanol to get the pure tyrosine hydrazine 4 with the yield of 71%. Finally, compound 4 (3.00 g, 15.0 mmol) was dissolved in dried THF (100 mL) under nitrogen atmosphere at the three-necked round bottom flask. 3-Isocyanatopropyltriethoxysilane (IPTES, 7.2 g, 30.0 mmol) was then added to the solution. The reaction mixtures were allowed to keep in a pre-heated oil bath at 40◦C for about 6 h. During the period, the reaction was monitored by TLC. The resulting white oil was collected through rotary evaporation. Then, the white oil was recrystallized by anhydrous hexane to afford TBOS as a highly viscous solid with the yield of 80%. The characterization of TBOS: ^{1}H-NMR(DMSO,400Hz,δ ppm):9.70(s, 1H, -NH-CO-), 9.20(s, 1H, -OH), 7.33(s, 1H, -NH-CO-),6.99-7.01(d, *J*=6.8Hz, 2H, ArH-),6.64-6.67 (d, *J*=6.8Hz, 2H, ArH-),6.26-6.29 (t, *J*=6.0Hz ,1H, -NH-CO-),6.14(t, *J*=6.2Hz, 1H),6.05(d, *J*=8.0Hz ,1H), 4.17(q, *J*=2.7Hz, 1H),3.71-3,76 (d, *J*=10.0Hz ,12H, -CH_2-O),2.90-3.00(m, 4H, -CH_2-),2.76-2.81 (q, *J*=9.0Hz ,1H, Ar-CH_2-) ,2.60-2.66 (q, *J*=12.0Hz ,1H, Ar-CH_2-), 1.36-1.44(m, 4H, -CH2-) , 1.12-1.16 (d, J=8.0Hz ,18H, -CH3), 0.48-0.53(m, 4H, -CH_2Si). ^{13}C NMR (400 MHz, $CDCl_3$, ppm) d 172.3, 157.9 157.7, 155.8, 130.0, 127.3, 114.8, 57.6, 53.6, 42.0 41.8, 36.0, 23.4 23.2, 18.1,7.2 7.2; ESI-MS: m/z = 689, m/z = 690 ($M+H^+$), m/z = 712 ($M+Na^+$); FT-IR (KBr, cm^{-1}): 3298.38 (Bz-OH), 2975.49(-CH3), 2928.40 (C-CH2-C), 2887.97 (-CH), 1652.09 (-CO-NH), 1567, 1517, 1450(Bz), 1080.23 (-O-Si-).

Preparation of Periodic mesoporous organosilicas materials with Tyrosine in the framework (Tyr-PMOs)

The materials of Tyr-PMOs were prepared by the co-condensation of TEOS and TBOS with the template P123 under the acid media, as shown in Scheme 3. In a typical synthesis, Pluronic P123 (2.0g) was firstly dissolved in the mixed solution of distilled water (15g) and HCl (60g 2M) at room temperature to obtain a clear solution. Then, on the basis of the molar ratios, the certain amount of TEOS and TBOS were added to the above homogenous solution under stirring at 40℃ for 24h. Thereafter, the mixtures were transferred into a stainless steel reactor with polytetrafluorethylene and heated at 100℃ for another 24h. Finally, the product was collected by filtration, washed with distilled water and dried in air under ambient conditions to get a yellowish solid powder. The template was extracted by refluxing 1.0g of as-synthesized materials in the mixtures of 300 mL ethanol and 10mL hydrochloric acid for 48h. Finally, the materials obtained were denoted as Tyr-PMOs-n, where n (n=2.5%, 5%, 7.5%, 10%, 15%) is the molar percent of TBOS/(TBOS+TEOS).

Characterization

The ^{1}H NMR experiment was recorded on a AC-400 Avance spectrometer at 25 °C, and DMSO was chosen as the solvent. All chemical shifts (d) are reported in parts per million (ppm) downfield from TMS; J values are given in hertz (Hz). The FT-IR spectra were collected on a Thermo Nicolet iS5 FT instrument in the range of 400-4000 cm^{-1} at 298 K, and the sample was mixed with KBr powder at a ratio of 10:90 (w/w). High resolution mass spectra were run on Aglient 6550 iFunnel Q-TOF. Small-angle X-ray diffraction (SAXRD) measurements were carried out on a ARL XTRA diffractometer equipped with Cu Kα radiation (λ= 1.5418 Å) sources at RT in a 2θ range (scattering angle) between 0.5° and 8°. The operating voltage and current of the X-ray tube were 40 kV and 20 mA, respectively. N_2 adsorption–desorption isotherms were obtained by using Micrometrics ASAP2020. Prior to testing, the samples were pre-treated at 373 K overnight in vacuum. The surface area was evaluated from Brunauer–Emmett–Teller (BET) method. The pore diameter and pore volume of samples were derived from the adsorption isotherm branch data using Barret–Joyner–Halenda (BJH) method. The total pore volume was determined from the amount adsorbed at a relative pressure of 0.99. The BJH pore diameter was defined as the maximum pore diameter on the pore size distribution curve. Transmission electron microscopic (TEM) images were collected by a JEOL JEM-200CX electron microscope. Scanning electron microscopy (SEM) characterisation was performed by using HITACHI TM-3000, and the samples were coated with Au film to improve the conductivity prior to imaging. ^{29}Si solid-state NMR experiments were carried out using a Bruker AVANCE III-500 spectrometer (BrukerBioSpin, Karlsruhe, Germany) operating at a magnetic field strength of 11.7 T, equipped with a 4 mm double-resonance MAS probe, which were collected at an 8 kHz

MAS spinning speed with a π/4 pulse width of 2.3μs and a recycle delay of 90s. UV-vis absorption spectra were collected on a UV 360 spectrophotometer (Shimazu, Japan).

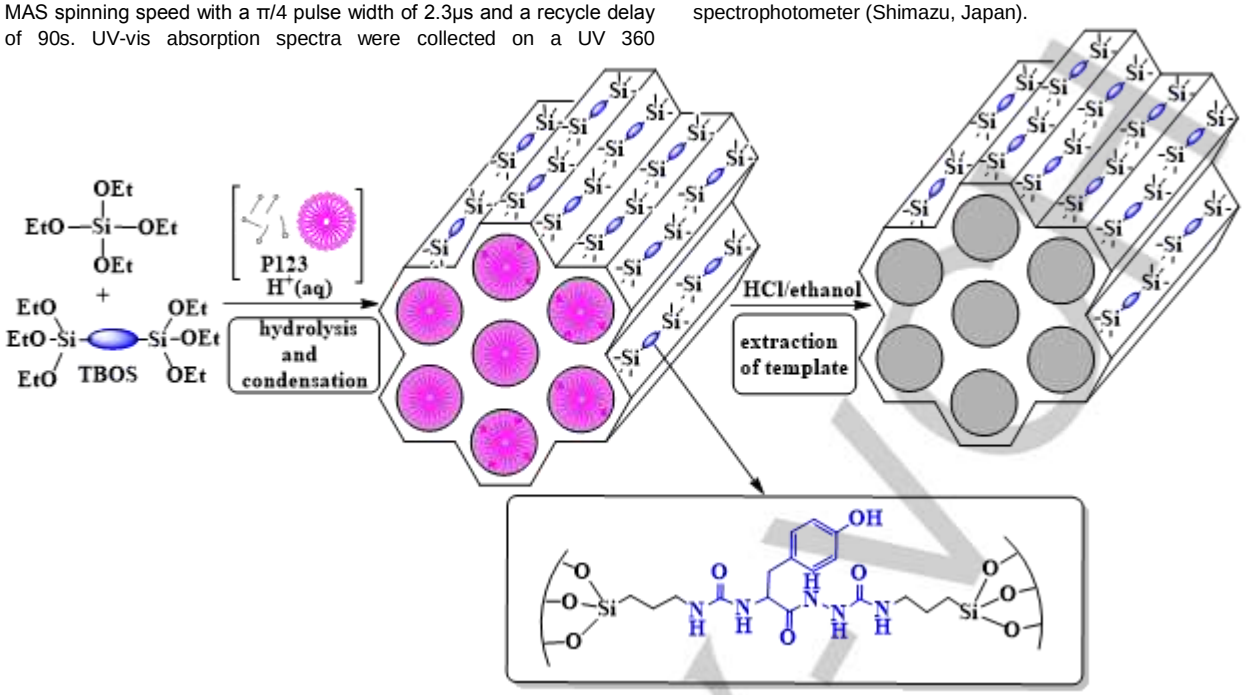

Scheme 3. Preparation of Periodic mesoporous organosilicas materials with the frame work of Tyrosine (Tyr-PMOs)

Immobilization of HRP on material of Tyr-PMOs

The typical procedure of immobilizing HRP on Tyr-PMOs is described as followings: 250 mg of Tyr-PMOs and 5.0 mL phosphate buffer solution of HRP with the concentration of 1mg mL-1 were shaken for 6h at 4◦C. The resulting product was filtered and washed with the same buffer solution to remove unattached enzyme. The obtained immobilized HRP on Tyr-PMOs was designated as Tyr-PMOs-n-HPR (n=2.5%, 7.5%, 10%, and 15%, where n is the molar percent of TBOS/(TBOS+TEOS)). In order to study the effects of different conditional parameters on immobilization of HRP, the experimental conditions including pH, temperature and time were considered respectively. The experiments were performed by adjusting one parameter but the other parameters were fixed in the immobilization of HRP on Tyr-PMOs.

The adsorbed amounts of HRP (q_t) was calculated from the mass balance equation as Eq.(1):

$$q_t = \frac{V(C_0 - C_t)}{W} \quad (1)$$

where c_0 is the initial concentration of solutions (mg mL-1) containing HRP, $c_t$is the concentration after immobilizing HRP (mg mL-1), V is the volume of solutions (mL) and W is the mass of Tyr-PMOs samples (mg). The HRP concentrations were analyzed in triplicate, and the experimental errors were within ±5%.

Measurement of enzymatic activities of free and immobilized enzyme

To determine the activity of free and immobilized enzyme HRP, two substrates of hydrogen peroxide and pyrogallolin were employed in the model reaction [38]. 0.5 mL of hydrogen peroxide (0.05 M) was mixed with the solutions of 2.4 mL phosphate buffer solution (pH 6.0) of pyrogalloland (0.013M). Then, the material of immobilized HRP (Tyr-PMOs-n-HRP, 5mg) was added into the above solutions, and the reaction was carried out at 30◦C for 1 min. After the reaction, the enzyme activity was determined by measuring the UV-vis absorbance of the product (purpurogallin) at 420 nm. The extinction coefficient of pyrogallol was found to be 0.0126 M-1cm-1at 420 nm. The assay of free HRP was performed under the same conditions as the materials of immobilized HPR were replaced with 5mg of free HRP. All of the samples were analyzed in triplicate. One unit of HRP activity was defined as the amount of HRP that released 1 mol per minute of oxidized product at pH 6.0, and 30 ◦C.

The enzyme activity was calculated according to Eq. (2):

$$\text{Enzyme activity } U = \frac{1000X}{t} \quad (2)$$

where x is absorbance, and t is enzymatic reaction time (min).

Stabilities of immobilized enzyme HRP on Tyr-PMOs

The storage stability was evaluated after all the samples of Tyr-PMOs-n-HRP with the maximum amounts of immobilized HRP were kept in room temperature at dried environment for a specified period of time. Subsequently, 2 mg of Tyr-PMOs-n-HRP were taken for activity assay. The operational stability of immobilized HRP was determined by using screened Tyr-PMOs-n-HRP with maximum loading amounts of enzyme to catalyze the reaction of the assay solution containing pyrogallol, phosphate buffer solution and H2O2 for eight cycles. After each cycle of reaction, Tyr-PMOs-n-HRP were collected and washed with phosphate buffer (0.1 M, pH 6.0) to remove any residual substrate. Next, Tyr-PMOs-n-HRP was transferred into fresh reaction medium and the retained activity was estimated. We considered the initial activity was 100% for the immobilized enzyme.

Acknowledgements

Financial supported by National Natural Science Foundation of China (No. 21106069) and the State Key Laboratory of Materials-Oriented Chemical Engineering (KL15-08) are gratefully acknowledged. The authors would like to thank Prof. Hailu Zhang of Suzhou Institute of Nano-tech and Nano-bionics, Chinese Academy of Sciences for the ^{29}Si solid-state NMR characterization and analysis.

Keywords: Periodic mesoporous organosilicas (PMOs) • Tyrosine bridged organosilicas • HRP • Immobilization of enzyme • Amino acid

[1] W. Na, W. Wei, J.N. Lan, Z.R. Nie, H. Sun, Q.Y. Li, *Microporous. Mesoorous. Mater.* **2010**,*134,* 72-78.
[2] C. H. Wong, G. M. Whitesides, Enzymes in Synthetic Organic Chemistry, Pergamon Press, Oxford, **1994.**
[3] S. A. Guila, R. V. Duhalt, R. Tinoco, M. Rivera, G. Pecchi, J. B. Alderete, *Green Chem.* **2008**, *10,* 647-653.
[4] A. Schmid, J. S. Dordick, B. Hauer, A. Kiener, M. Wubbolts, B. Witholts, *Nature,* **2001**, *409,* 258-268.
[5] V. V. Mozhaev, M. V. Sergeeva, A. B. Belova, Y. L. Khmelnitsky, *Biotechnol. Bioeng.* **1990**, *35,* 653-659.
[6] S. G. Burton, D. A. Cowan, J. M. Woodley, *Nat. Biotechnol.* **2002**, *20,* 37-45.
[7] M. Hartmann, *Chem. Mater.* **2005**, *17,* 4577-4593.
[8] P. McMorn, G. J. Hutchings, *Chem. Soc. Rev.* **2004**, *33,* 108-122.
[9] S. Hudson, J. Cooney, B. K. Hodnett, E. Magner, *Chem. Mater*. **2007**, *19,* 2049-2055
[10] M. Kapoor, R. C. Kuhad, *Appl. Biochem. Biotechnol.* **2007**, *142,* 125-138.
[11] S. Chen, N. Song, X. Liao, B. Shi, *Chin. J. Biotechnol.* **2011**, *27,* 1076-1081.
[12] M. Namdeo, S. K. Bajpai, *J. Mol. Catal. B-Enzym.* **2009**, *59,* 134-139.
[13] Y. K. Chang, L. Chu, *Biochem. Eng. J.* **2007**, *35*, 37-47.
[14] L. Huang, Z. M. Cheng, *Chem. Eng. J.* **2008,** *144,* 103-109.
[15] M. Soleimani, A. Khani, K. Najafzadeh. *J. Mol. Catal. B-Enzym* **2011**, *74,* 1-5.
[16] K. Ramani, S. Karthikeyan, R. Boopathy, L. J. Kennedy, A. B. Mandal, G. Sekaran, *Process. Biochem*. **2012**, *47,* 435-445.
[17] H. P. Y. Humphrey, A. W. Paul, *J. Mater. Chem.* **2005**, *15,* 3690-3700.
[18] E. Weber, D. Sirim, T. Schreiber, B. Thomas, J. Pleiss, M. Hunger, R. Gläser, V. B. Urlacher, *J. Mol. Catal. B: Enzym.* **2010**, *64,* 29-37.
[19] Y. Wang, K. Wang, J. Zhao, X. Liu, J. Bu, X, Yan, R. Huang, *J. Am. Chem. Soc.* **2013**, *135,* 4799-4804.
[20] F. Hoffmann, M. Cornelius, J. Morell, M. Fröba, *Angew. Chem. Int. Ed.* **2006**, *45,* 3216-3251.
[21] M. C. Burleigh, M. A. Markowitz, M. S. Spector, B. P. Gaber, *J. Phys. Chem. B.* **2001**, *105,* 9935-9942.
[22] W. J. Hunks, G. A. Ozin, *J. Mater. Chem.* **2005**, *15,* 3716-3724.
[23] J. G. Croissant, Y. Fatieiev, K. Julfakyan, J. Lu, A. H. Emwas, D. H. Anjum, H. Omar, F. Tamanoi, J. I. Zink, N. M. Khashab, *Chem. Eur. J.* **2016**, *22*, 14806-14811
[24] S. Z. Qiao, C. Z. Yu , W. Xing, Q. H. Hu, H. Djojoputo, G. Q. Lu. *Chem. Mater.* **2005**, *17*, 6172-6176.
[25] S. Hudson, E. Magner, J. Cooney, B. K. Hodnett, *J. Phys. Chem. B* **2005**, *109*, 19496-19506 .
[26] M. Park, S. S. Park, M. Selvaraj, D. Zhao, C. Ha, *Microporous. Mesoorous. Mater.* **2009**, *124,* 76-83.
[27] E. Serra, E. Díaz, I. Díaz, R. M. Blanco, *Mesoporous. Mater,* **2010**, *132,* 487-493.
[28] O. J. D'Souza, R. J. Mascarenhas, A. K. Satpati, L. V. Aiman, Z. Mekhalif, *Ionics*, **2016**, *22*, 405-414.
[29] P. H. Pacheco, P. Smichowski, G. Polla, L. D. Martinez, *Talanta* **2009**, *79*, 249-253.
[30] B. R. White, B. T. Stackhouse, J. A. Holcombe, *J. Hazard. Mater,* **2009**, *161*, 848-853
[31] L. Maggini, L. Travaglini, I. Cabrera, P. C. Hartmann, L. D. Cola, *Chem. Eur. J.* **2016**, *22*, 3697-3703
[32] U. Yogeswaran, S. Thiagarajan, S. M. Chen, *Carbon*, **2007**, *45,* 2783-2796.
[33] D. C. Culita, G. Marinescu, L. Patron, O. Carp, C. B. Cizmas, L. Diamandescu, *Mater. Chem. Phys,* **2008**, *111,* 381-385.
[34] M. S. Moorthy, S. S. Park, F. P. Dong, S. H. Hong, M. Selvaraj, C. S. Ha, *J. Mater. Chem.* **2012,** *22,* 9100-9108
[35] H. Essa, E. Magner, J. Cooney, B. K. Hodnett, *J. Mol. Catal. B: Enzym,* **2007**, *49,* 61-68.
[36] J. Ho, M. K. Danquah, H. T. Wang, G. M. Forde, *J. Chem. Technol. Biotechnol,* **2008**, *83*, 351-358.
[37] A. Henriksen, D. J. Schuller, K. Meno, A. T. Smith, M. Gajhede, *Biochemistry*, **1998**, *37*, 8054-8060.
[38] B. Halpin, R. Pressey, J. Jen, M. Mondy, *J. Food Sci.* **1989**, *54,* 644-649.

10.1002/asia.201701285

Entry for the Table of Contents (Please choose one layout)

Layout 1:

FULL PAPER

Novel periodic mesoporous organosilicas with tyrosine framework (Tyr-PMOs) was constructed. Incorporation of the tyrosine units in the framework, and phenolic hydroxyl group as binding center introduced within the channels at the same time. Long storage time and conventional stability of Tyr-PMOs after inmmobilizing HRP were found.

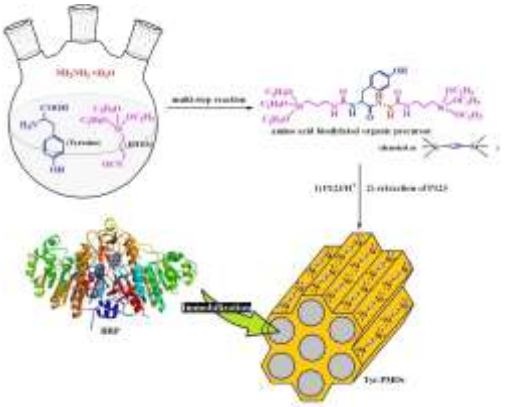

Wang Jianqiang[a], Zhang Wenqi[a], Gu Changqing[a], Zhang Wenpei[a], Zhou Man[a], Wang Zhiwei[a], Guo Cheng*[a] and Sun Linbing[b]*

Page No. – Page No.

Step-up synthesis of periodic mesoporous organosilicas with the framework of tyrosine (Tyr-PMOs) and performance on horseradish peroxidase immobilization